Journal of the European Ceramic Society 22 (2002) 769–775

www.elsevier.com/locate/jeurceramsoc

Tensile creep behavior of a ytterbium silicon oxynitride–silicon nitride ceramic

Jian-Wu Cao[a], Akira Okada[a,*], Naoto Hirosaki[b]

[a]*Japan Fine Ceramics Center, Nagoya, 456-8587 Japan*
[b]*National Research Institute for Inorganic Materials, Tsukuba, 305-0044 Japan*

Received 10 January 2001; received in revised form 26 April 2001; accepted 20 May 2001

Abstract

Tensile creep behavior of hot pressed silicon nitride on the Si_3N_4–$Yb_4Si_2O_7N_2$ tie line was investigated at temperatures of 1300 and 1400 °C under an applied stress of 125 to 200 MPa. During the tests, the creep strain increased with time and the creep rate monotonically decreased both with time and strain. On the basis of minimum strain rates, the stress exponents for 1300 and 1400 °C were determined to be 3.1 and 1.7, respectively. All the specimens tested at 1400 °C lead to failure while exhibiting a large scatter in the time-to-failure data. The activation energy was determined to be 879 kJ/mol from a comparison between creep rates at different temperatures. The creep mechanism is discussed on the basis of the creep parameters and creep damage observation. © 2002 Published by Elsevier Science Ltd.

Keywords: Creep; Electron microscopy; Si_3N_4; Tensile creep

1. Introduction

Silicon nitride ceramics have attracted considerable attention due to their excellent high temperature properties, and extensive work has been carried out regarding applications requiring high temperature mechanical components, such as turbochargers and gas turbines. Silicon nitrides are often sintered with oxide additives, which react with both the silicon nitride matrix and silicon oxide present on the surfaces of grains, so that a liquid phase is formed at elevated temperatures. This liquid promotes densification via a liquid phase sintering mechanism and forms a secondary phase on cooling at the grain boundaries. The mechanical properties of sintered ceramics at high temperature are influenced by the nature of the secondary phase. Control of the grain boundaries is therefore important for developing silicon nitride ceramics having excellent mechanical properties at high temperatures.

Reducing the amount of grain boundary phases and using refractory grain boundary phases are general approaches for developing silicon nitrides for high temperature applications. Pressure sintering, such as hot pressing and hot isostatic pressing, is an effective means for densifying silicon nitrides while reducing the amount of sintering additives. Chemical control of the liquid phase can eliminate or reduce the amount of glassy phase via crystallization after sintering and dissolution into silicon nitride grains by forming a solid solution. Gas-pressure sintering can suppress the decomposition of silicon nitride by using a nitrogen overpressure and it is thereby possible to use refractory sintering additives due to the high temperatures involved.

Rare earth oxides have been intensively used as refractory sintering aids to achieve densification of silicon nitride while maintaining excellent high temperature mechanical properties[1,2]. The densification behavior and high temperature mechanical properties depend on the type of rare earth oxides used to form the secondary phases. A material with a composition close to the Si_3N_4–$Yb_2Si_2O_7$ tie line was reported to have 99.5% theoretical density when sintered at 1850 °C for 4 h under 1.8 MPa of nitrogen gas[3], and exhibited excellent creep resistance at 1400 °C in flexural creep tests.[4] The secondary phase in Yb_2O_3-doped silicon nitride depends on the chemical composition, but a $Yb_2Si_2O_7$ phase is commonly chosen.[5,6] The fabrication of hot pressed

* Corresponding author. Present address: Materials Research Laboratory, Nissan Motor Co., Ltd., Yokosuka, 237-8523 Japan.
E-mail address: okada-a@mail.nissan.co.jp (A. Okada).

0955-2219/02/$ - see front matter © 2002 Published by Elsevier Science Ltd.
PII: S0955-2219(01)00340-5

silicon nitride on the Si_3N_4–$Yb_4Si_2O_7N_2$ tie line has also been reported.[7] This material also exhibits excellent creep resistance in compression.[8] It should be noted that the tensile creep rate in silicon nitride is, however, much greater than in compression due to intensive cavitation occurring in tension, and that the stress exponent value is usually higher in tension than compression.[9–13] The difference in the amount of cavitation between tension and compression is thought to be responsible for the strong asymmetry in creep behavior.[10] The objective of the present investigation is thus to investigate the tensile creep and creep rupture behavior of silicon nitride containing an oxynitride phase of $Yb_4Si_2O_7N_4$.

2. Experimental procedure

2.1. Material

The starting materials were Si_3N_4 (alpha-type, SN-E10, UBE Industries, Tokyo, Japan), SiO_2 (99.9%, Koujundo Chemical Lab Co., Ltd., Saitama, Japan) and Yb_2O_3 (99.9%, Shin-Etsu Chemical Co. Ltd., Tokyo, Japan). The powders, having an overall chemical composition of 97.6 mol% Si_3N_4 and 2.4 mol% $Yb_4Si_2O_7N_4$, were ground together in ethyl alcohol using a planetary ball mill for 2 h.[7] After drying with a rotation evaporator and sieving, the powder mixtures were hot pressed at 1750 °C for 1 h under a pressure of 200 MPa in nitrogen gas at a pressure of 0.925 MPa. The dimensions of hot pressed specimens were approximately $80\times45\times5$ mm^3 and the resulting relative density was 98 to 99% for four samples. The crystalline phases in the material determined by X-ray diffraction were β-Si_3N_4 and $Yb_4Si_2O_7N_2$. Fig. 1 shows the microstructures of the material, indicating that the material consists of elongated grains in a matrix of fine grains. The average length of the elongated grains was 5 to 10 μm. Table 1 lists the four-point flexural strength of the material investigated at several temperatures. The flexural strength was measured using specimens having dimensions of $3\times4\times40$ mm^3. The crosshead speed was 0.5 mm/min, and the inner and outer spans were 10 and 30 mm, respectively.

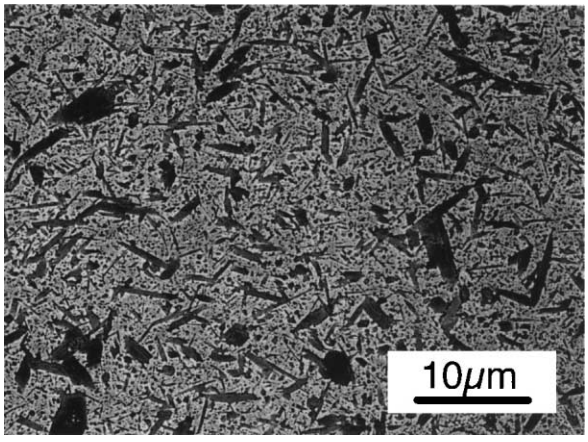

Fig. 1. Microstructure of the investigated material consisting of Si_3N_4–2.4 mol% $Yb_4Si_2O_7N_4$.

2.2. Tensile creep test

Fig. 2 shows a flat dog-bone specimen used for tensile creep testing. The total length of each specimen was 70 mm, with a rectangular cross section of 4.0×2.5 mm^2 in the gauge area. The gauge length was 20 mm.

Creep tests were performed in air using a dead-weight loading apparatus, HTT-300 (Toshin Kogyo Co., Ltd., Tokyo, Japan). The specimens were fixed in hot grips using four silicon carbide pins connected to silicon carbide loading fixtures. The test furnace had six heating elements of $MoSi_2$ and the temperature was controlled to within 5°. Displacement of the inner positions of the hot grips was measured with an optical image analyzer VAD-1R (Toshin Kogyo Co., Ltd., Tokyo, Japan). Prior to the tests, four strain gauges were glued on to the four planes in the gauge area of the specimen and adjusted to reduce the bending strain of the specimen. The four plane strains, ϵ_1, ϵ_2, ϵ_3, and ϵ_4, were measured with a strain amplifier, where the subscripts 1 and 2 correspond to the opposite planes of 3 and 4, respectively. The bending strain expressed as percent bending was adjusted to be lower than 5% at a stress of 60 MPa at room temperature. It should be noted that it is important to choose a suitable combination of pin diameters in order to reduce the bending strain in the traverse direction when the tensile load is applied through

Table 1
Four-point flexural strength of silicon nitride used in the present study

RT	1200 °C	1400 °C	1500 °C
1307 MPa	990 MPa	700 MPa	418 MPa

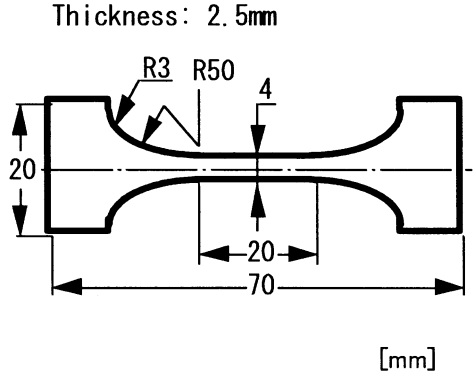

Fig. 2. Flat dog-bone specimen used for tensile creep test.

the shoulders of the dog-bone specimens. The percent bending, PB, is defined as[14]

$$PB = \frac{\varepsilon_b}{\varepsilon_0}\ 100 \quad (1)$$

where

$$\varepsilon_b = \left[\left(\frac{\varepsilon_1 - \varepsilon_3}{2}\right)^2 + \left(\frac{\varepsilon_2 - \varepsilon_4}{2}\right)^2\right]^{1/2}$$

$$\varepsilon_0 = \frac{\varepsilon_1 + \varepsilon_2 + \varepsilon_3 + \varepsilon_4}{4}$$

Specimens were heated under a pre-load of 98 N with a heating rate of 15 °C/min. After reaching the test temperature, the temperature was maintained for about 15 min to ensure a uniform temperature gradient. The test load was then applied and the creep test started. Details of the experimental technique are described elsewhere.[15–20]

2.3. Transmission electron microscopy

The microstructure after creep was examined with a transmission electron microscope (EM-002B, Topcon Co., Ltd., Tokyo, Japan) at an accelerated voltage of 200 kV. Samples were cut from the crept specimens so as to be observed on the plane parallel to the tensile axis.

3. Results and discussion

Fig. 3 shows creep curves at 1300 and 1400 °C. All the specimens tested at 1400 °C failed and the failure times were several tens of hours. The tests at 1300 °C were continued for several hundreds of hours and interrupted prior to failure. As listed in Table 2, the failure strains in the creep tests at 1400 °C were 0.029 at 160 MPa, 0.020 at 150 MPa, 0.038 at 145 MPa, 0.031 at 137 MPa and 0.027 at 125 MPa. At both temperatures, the creep rate increases with an increase in the applied stress. Note that transient creep followed by steady-state like creep was always seen in the present study and the tertiary stage was not observed. This is consistent with typical creep curves previously reported for silicon nitrides[21–23]

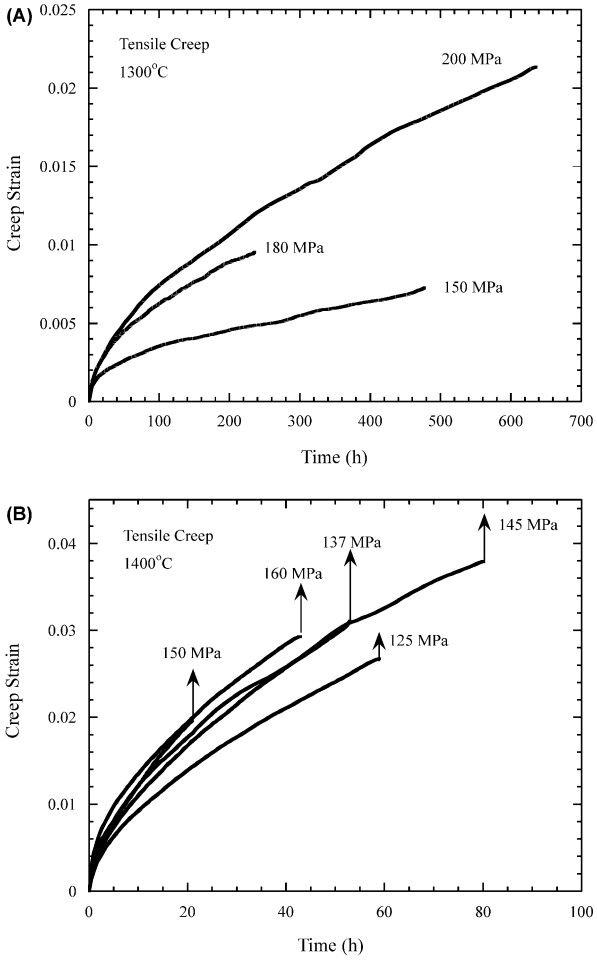

Fig. 3. Tensile creep curves obtained at the indicated stresses at (A) 1300 °C and (B) 1400 °C.

Figs. 4 and 5 show the time and strain dependences of strain rates, respectively. It is clear that the creep rate

Table 2
Summarized creep data in the present study

Specimen	Creep condition			Creep test results			
	Temperature (°C)	Test load (N)	Stress (MPa)	Time interrupted (h)	Time-to-rupture (h)	Failure strain	Minimum stress rate (s^{-1})
1	1300	1502.8	150.0	477			2.47×10^{-9}
2	1300	1832.6	179.8	236			5.33×10^{-9}
3	1300	2033.5	200.0	636			5.79×10^{-9}
4	1400	1259.3	124.9		59	0.027	8.41×10^{-8}
5	1400	1381.8	136.9		53	0.031	1.07×10^{-7}
6	1400	1504.3	150.2		21	0.020	1.76×10^{-7}
7	1400	1489.6	145.0		80	0.038	7.48×10^{-8}
8	1400	1641.5	160.0		43	0.029	1.17×10^{-7}

monotonically decreases with time and creep strain in all the tests at both 1300 and 1400 °C. Therefore, the minimum of the strain rate appears at the end of the creep tests. This indicates that the rupture time influences the minimum strain rate. According to Norton's law, the creep rate in the steady state stage, $\dot{\varepsilon}$, may be expressed as a power function of stress σ.

$$\dot{\varepsilon} = D_0 \exp\left(-\frac{Q}{RT}\right)\sigma^n \tag{2}$$

where n is the stress exponent, R is the gas constant, T is the absolute temperature and Q is the activation energy. Fig. 6 shows stress exponents obtained from the minimum strain rate data, namely $n = 3.1$ at 1300 °C and $n = 1.7$ at 1400 °C. Since the strain rate data were obtained from the final part of the creep curves, the shorter failure and interrupted times lead to greater values in the minimum strain rates. For example, the plot of the creep test under a stress of 180 MPa at 1300 °C appears slightly above the solid line in Fig. 6 because it corresponds to the shortest interrupted time.

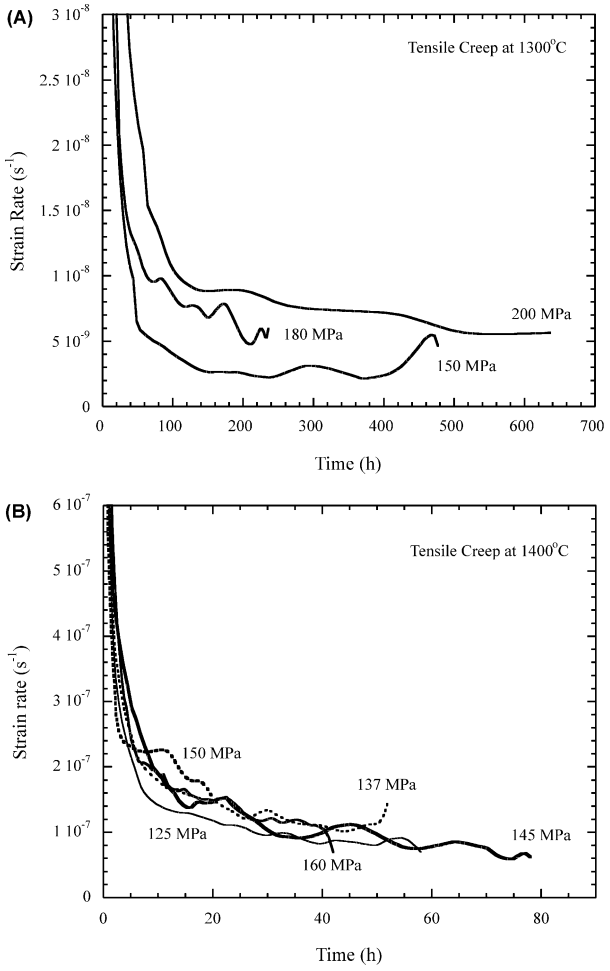

Fig. 4. Tensile creep strain rate dependence on creep time at (A) 1300 °C and (B) 1400 °C.

For the plots at 1400 °C, the shortest time-to-failure was obtained for the test at 150 MPa and the corresponding minimum strain rate was just above the solid line. Furthermore, the minimum strain rate to the longest

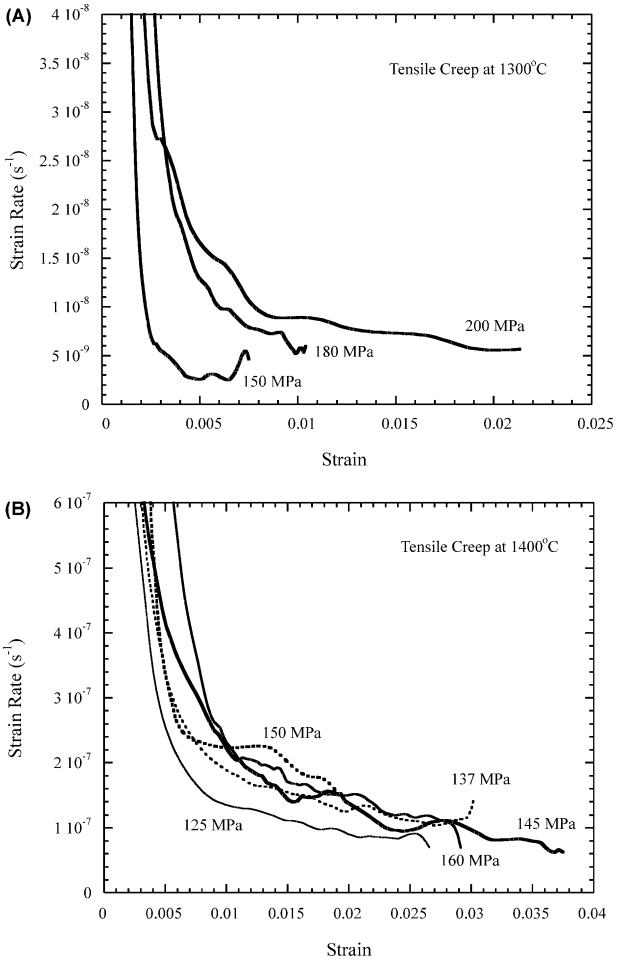

Fig. 5. Tensile creep strain rate versus creep strain at (A) 1300 °C and (B) 1400 °C.

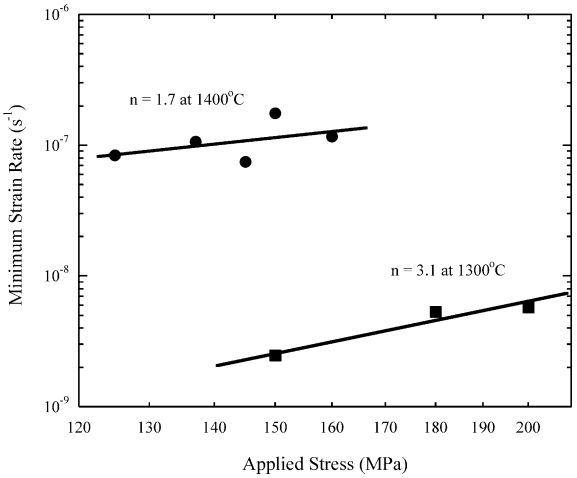

Fig. 6. Tensile creep strain rate versus applied stress at 1300 °C and 1400 °C.

time-to-failure for the test at 145 MPa was situated just below the line.

The apparent stress exponent can be determined from constant time and strain plots; for constant time plots, it was reported that the stress exponent calculated from the strain rate at constant time is lower than that determined from the minimum strain rate, while in constant strain plots, higher n values are obtained at small creep strains[24] Such a trend was, however, unclear in the present study due to the limited stress range in the creep tests.

The activation energy can be obtained from a comparison of strain rates at different temperatures. From direct comparison between the minimum strain rates at 150 MPa, the activation energy was calculated to be $Q = 934$ kJ/mol. Since the strain rates were obtained from the final stages of the creep tests and the strain rates were decreasing gradually with creep time, the calculated value of the activation energy may involve considerable error. In fact, the value seems to be overestimated, assuming that the minimum strain rate at 1400 °C is overestimated because the data point was obtained from the shortest time-to-failure in the series of creep tests (see the data point at 150 MPa in Fig. 6). When the values of the minimum strain rates at 150 MPa were estimated from the interpolation of the solid lines in Fig. 6, the activation energy was calculated to be 879 kJ/mol. Since the stress exponents vary between the two test temperatures, the activation energy depends on the applied stress. Accordingly, the activation energy, calculated from two data points at two temperatures, slightly decreases with an increase in the applied stress.

It was reported that a compression creep test of this material was conducted at 1370 °C under a stress of 200 MPa, and that the steady-state creep rate was about 1×10^{-8} s^{-1}.[8] Although there are no available tensile creep data corresponding to the same test conditions, the creep rate in tension corresponding to these compression creep conditions can be estimated from the present data. This estimate indicates that tensile creep rate is about ten times higher than compression. This difference is consistent with a direct comparison between tension and compression.[10] Furthermore, the stress exponent in compression at 1370 °C was around 1.5,[8] and this is close to the value under tensile creep at 1400 °C in the present study. This suggests that the dominant creep mechanism is identical both in tension and compression while tensile stress enhances the creep rate.

Fig. 7 shows the relationship between time-to-rupture and the applied stress at 1400 °C. The time-to-rupture decreases with an increase in stress. Time-to-failure t_f may be described by the power function of stress σ:

$$t_f = B\sigma^{-N} \tag{3}$$

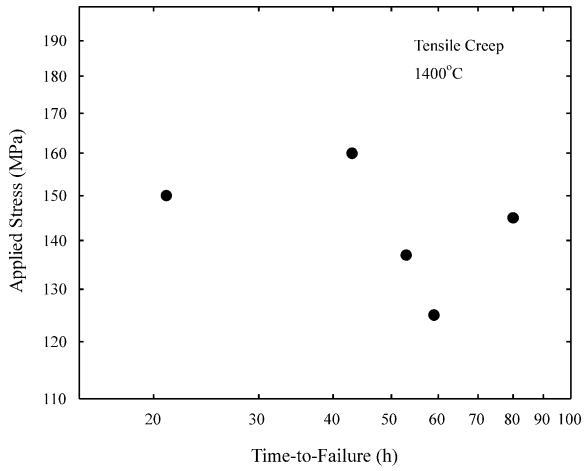

Fig. 7. Time-to-failure and applied stress of silicon nitride at 1400 °C.

where N is a parameter describing stress–rupture behavior. In the present study, the N value was difficult to determine due to the large scatter in data.

Fig. 8 shows the minimum strain rates $\dot{\varepsilon}_{\min}$ against time-to-failure. The strain rate decreases with an increase in the time-to-failure. The slope gives a Monkman–Grant parameter of $m = 1.54$, which is defined by:[25]

$$t_f = C\dot{\varepsilon}_{\min}^{-m} \tag{4}$$

The m value obtained is consistent with the previous work since it is somewhat greater and close to one.[22]

A variety of creep mechanisms occur in silicon nitride at high temperatures. Viscous flow is often responsible for the initial deformation through the rearrangement of the grain boundary glassy phase[26,27] and the solution–precipitation mechanism can be responsible for further deformation.[28] However, the stress exponents in tensile creep tests of silicon nitride are sometimes very large, and extensive cavitation contributes to the major deformation.[10,29,30] Therefore, tensile creep in the steady state in general seems to be mainly a combination of

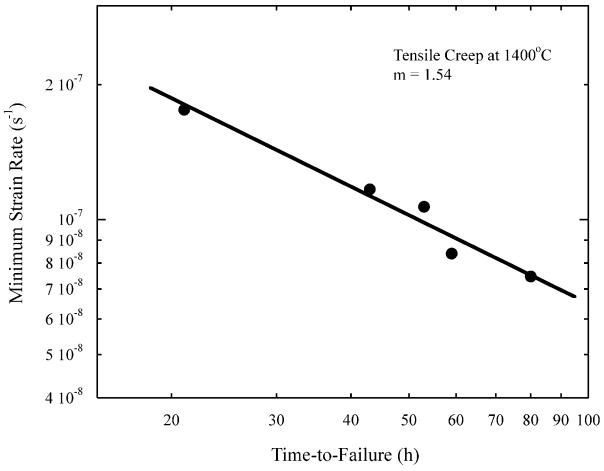

Fig. 8. Time-to-failure and strain rate of silicon nitride at 1400 °C.

two mechanisms: the solution–precipitation mechanism and cavitation creep. Since the intensive cavitation that occurs during tensile creep accelerates the creep rate, new expressions for cavitation creep have been proposed.[12,13] Assuming that the greater contribution of cavitation creep leads to the higher stress exponent, the stress exponent may be a way of evaluating the contribution of cavitation.[29,30] The activation energy should also be different between the two mechanisms. Fig. 9 shows plots of activation energy Q against the n value, taken from various data already published.[21,31–42] It is clear that a large n value corresponds to high activation energy with two exceptional data points, marked as 6 and 14. However, data point number 14 was explained as being the crack growth exponent.[41] Moreover, data point 6 results from the SiO_2 rich grain boundary phase since this data point corresponds to the compression creep data of the material on the Si_3N_4–Si_2N_2O tie line[35,36] Therefore, these data points may be exceptional and the activation energy and the stress exponent of creep deformation seem to strongly correlate with each other. Note that the present data point is placed along the trend of the previous data points when the activation energy is determined from interpolated values and the stress exponent is chosen to be 2.4 for the average over the values for two temperatures.

Fig. 10 shows a transmission electron micrograph of the crept specimen, which was tested at 1400 °C under a stress of 137 MPa with a time-to-failure of 53 h. This indicates that the material consists of silicon nitride crystals of irregular shape. The secondary phase present at triple junctions looks dark and cavities can hardly be seen. This suggests that cavitation is most likely not the dominant deformation mechanism of this material at 1400 °C, unlike the usual class of silicon nitrides. This observation is also consistent with the relatively low stress exponent value of 1.7 in tension.

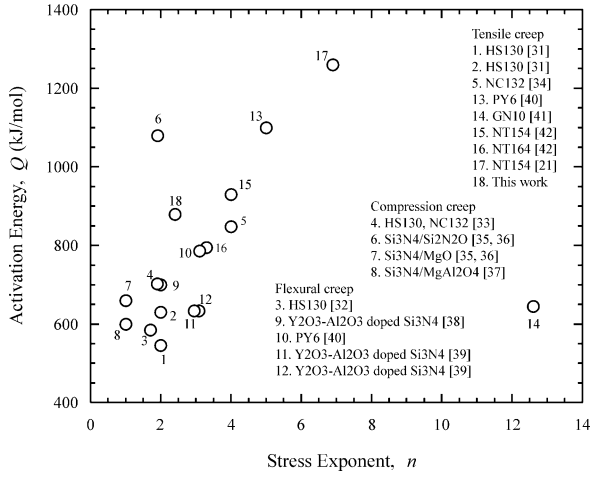

Fig. 9. The activation energy and stress exponent n for various creep tests.

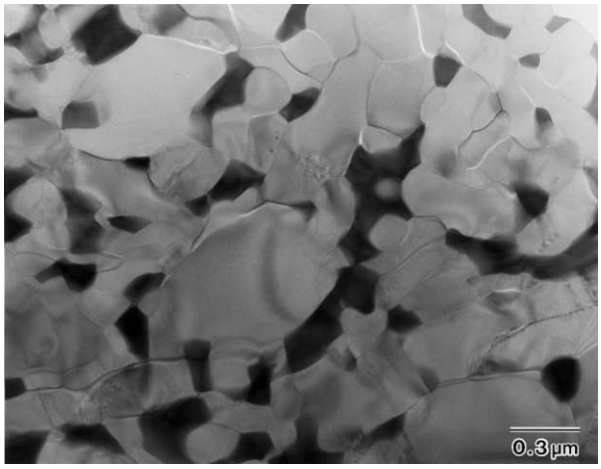

Fig. 10. Transmission electron micrograph of Yb-doped silicon nitride crept at 1400 °C for 53 h under a stress of 137 MPa. Bright image shown indicating that material consists of silicon nitride crystals having irregular shape. The secondary phase present at triple junctions looks dark and cavities are hardly seen.

4. Summary

Tensile creep behavior of silicon nitride, sintered with additions of Yb_2O_3 and SiO_2 to give a theoretical secondary phase composition of 2.4 mol% $Yb_4Si_2O_7N_4$, was investigated. The material contained crystalline phases of β-Si_3N_4 and $Yb_4Si_2O_7N_4$. Considerable creep deformation was observed during tests at temperatures of 1300 and 1400 °C, and the strain rate monotonically decreased with time and strain. The stress exponent determined from the minimum strain rate was 3.1 at 1300 °C and 1.7 at 1400 °C. TEM observation revealed that cavitation is not the dominant creep mechanism in this case, and this observation was consistent with the relatively low stress exponent value in tension.

Acknowledgements

The authors would like to thank Mr. T. Suzuki for assisting with TEM work and Mr. Y. Yamamoto for preparing specimens. The work was conducted under the High Temperature Materials 21 project, promoted by the Science and Technology Agency of Japan.

References

1. Sanders, W. A. and Mieskowski, D. M., Strength and microstructure of sintered Si_3N_4 with rare-earth-oxide additions. *Am. Ceram. Soc. Bull.,* 1985, **62**, 304–309.
2. Hirosaki, N., Okada, A. and Matoba, K., Sintering of Si_3N_4 with the addition of rare-earth oxides. *J. Am. Ceram. Soc.,* 1988, **71**, C–144-C-147.
3. Cinibulk, M. K., Thomas, G. and Johnson, S. M., Fabrication and secondary-phase crystallization of rare-earth disilicate-silicon nitride ceramics. *J. Am. Ceram. Soc.,* 1992, **75**, 2037–2043.

4. Cinibulk, M. K., Thomas, G. and Johnson, S. M., Strength and creep behavior of rare-earth disilicate-silicon nitride ceramics. *J. Am. Ceram. Soc.,* 1992, **75**, 2050–2055.
5. Vetrano, J. S., Kleebe, H.-J., Hampp, E., Hoffmann, M. J., Ruhle, M. and Cannon, R. M., Yb_2O_3-fluxed sintered silicon nitride: part 1, microstructure characterization. *J. Mater. Sci.,* 1993, **28**, 3529–3538.
6. Kleebe, H.-J., Bruley, J. and Ruhle, M., HREM and AEM studies of Yb_2O_3-fluxed silicon nitride ceramics with and without CaO addition. *J. Eur. Ceram. Soc.,* 1994, **14**, 1–11.
7. Nishimura, T., Mitomo, M and Suematsu, H., High temperature strength of silicon nitride ceramics with ytterbium silicon nitride. *J. Mater. Res.,* 1997, **12**, 203–209.
8. Yoshida, H., Ikuhara, Y., Sakuma, T., Nishimura, T. and Mitomo, M., High-temperature creep resistance in Yb_2O_3-fluxed Si_3N_4. In *Creep and Fracture of Engineering Materials and Structures*, ed. J. C. Earthman and F. A. Mohamed. The Minerals, Metals and Materials Societies, 1997, pp. 653–662.
9. Luecke, W. E., Wiederhorn, S. M., Hockey, B. J., Krause, R. F. and Long, G. G., Cavitation contributes substantially to tensile creep in silicon nitride. *J. Am. Ceram. Soc.,* 1995, **78**, 2085–2096.
10. Lofaj, F., Okada, A. and Kawamoto, H., Cavitational strain contribution to tensile creep in vitreous bonded ceramics. *J. Am. Ceram. Soc.,* 1997, **80**, 1619–1623.
11. Krause, R. F., Jr., Luecke, W. E., French, J. D., Hockey, B. J. and Wiederhorn, S. M., Tensile creep and rupture of silicon nitride. *J. Am. Ceram. Soc.,* 1999, **82**, 1233–1241.
12. Luecke, W. E. and Wiederhorn, S. M., A new model for tensile creep of silicon nitride. *J. Am. Ceram. Soc.,* 1999, **82**, 2769–2778.
13. Wereszczak, A. W., Ferber, M. K., Kirkland, T. P., Barnes, A. S., Frome, E. L. and Menon, M. N., Asmmetric tensile and compressive creep deformation of hot-isostatically-pressed Y_2O_3-doped Si_3N_4. *J. Eur. Ceram. Soc.,* 1998, **19**, 227–237.
14. Standard test method for elevated temperature tensile creep strain, creep strain rate, and creep time-to-failure for advanced monolithic ceramics. *ASTM Designation: C 1291–95*, The American Society for Testing and Materials, Philadelphia, PA, USA, 1995.
15. Lofaj, F., Usami, H., Okada, A. and Kawamoto, H., Long-term creep damage development in a self-reinforced silicon nitride. In *Engineering Ceramics '96: Higher Reliability Through Processing*, ed. C. N. Babini, M. Haviar and P. Sajgalih. Kluwer Academic Publishers, Dordrecht, The Netherlands , 1997, pp. 337–352.
16. Lofaj, F., Cao, J.-W., Okada, A. and Kawamoto, H., Comparison of creep behavior and creep damage mechanisms in the high-performance silicon nitrides. In *6th International Symposium on Ceramic Materials and Components for Engines*, ed. K. Niihara, S. Kanzaki, S. Komeya, K. Hirano and K. Morinaga. Technoplaza, Tokyo, Japan, 1997, pp. 713–718.
17. Lofaj, F., Okada, A. and Kawamoto, H., Creep damage in an advanced self-reinforced silicon nitride: part I, cavitation in the amorphous boundary phase. *J. Am. Ceram. Soc.,* 1999, **84**, 1009–1019.
18. Okada, A. and Lofaj, F., Elastic degradation of an advanced silicon nitride during tensile creep. *J. Eur. Ceram. Soc.,* 2000, **20**, 1521–1525.
19. Okada, A., Cao, J.-W. and Lofaj, F., Creep lifetime prediction for advanced silicon nitrides in 300 kW ceramic gas turbine. In *Proceedings of the International Symposium on Environment Conscious Materials—Ecomaterials*, ed. H. Mostaghaci. The Canadian Institute of Mining, Metallurgy and Petroleum, Ottawa, Canada , 2000, pp. 741–755.
20. Cao, J.-W., Okada, A. and Hirosaki, N., Creep and stress-rupture behavior of Y_2O_3-Nd_2O_3-doped silicon nitrides with different additive contents. Submitted to *J. Eur. Ceram. Soc.,* 2001, **22**(2), 237–245.
21. Wiederhorn, S. M., Hockey, B. J., Cranmer, D. C. and Yeckley, R., Transient creep behaviour of hot isostatically pressed silicon nitride. *J. Mater. Sci.,* 1993, **28**, 445–453.
22. Menon, M. N., Fang, H. T., Wu, D. C., Jenkins, M. G., Ferber, M. K., More, K. L., Hubbard, C. R. and Nolan, T. A., Creep and stress rupture behavior of an advanced silicon nitride: part I, experimental observation. *J. Am. Ceram. Soc.,* 1994, **77**, 1217–1227.
23. Menon, M. N., Fang, H. T., Wu, D. C., Jenkins, M. G. and Ferber, M. K., Creep and stress rupture behavior of an advanced silicon nitride: part II, creep rate behavior. *J. Am. Ceram. Soc.,* 1994, **77**, 1228–1234.
24. Grathwohl, G., Regimes of creep and slow crack growth in high-temperature rupture of hot-pressed silicon nitride. In *Material Science Research Vol. 18, Deformation of Ceramic Materials II*, ed. R. E. Tressler and R. C. Bradt. Plenum Press, New York, 1984, pp. 573–586.
25. Monkman, F. C. and Grant, N. J., An empirical relationship between rupture life and minimum strain rate in creep-rupture tests. *Proc. Am, Soc. Test. Mater.,* 1956, **56**, 593–630.
26. Chadwick, M. M., Jupp, R. S. and Wilkinson, D. S., Creep behavior of a sintered silicon nitride. *J. Am. Ceram. Soc.,* 1993, **76**, 385–396.
27. Wilkinson, D. S., Creep mechanisms in multiphase ceramic materials. *J. Am. Ceram. Soc.,* 1998, **81**, 1217–1227.
28. Raj, R. and Chyung, C. K., Solution-precipitation creep in glass ceramics. *Acta Metall.,* 1981, **29**, 159–166.
29. Morgan, P. E. D., Lange, F. F., Clarke, D. R. and Davis, B. I., A new Si_3N_4 materials: phase relations in the system Si–Sc–O–N and preliminary property studies. *J. Am. Ceram. Soc*., 1981, **64**, 1981, C-77–C-78.
30. Chen, C. F., Weiderhorn, S. M. and Chuang, T. J., Cavitation damage during flexural creep of sialon–YAG ceramics. *J. Am. Ceram. Soc.,* 1991, **74**, 1658–1662.
31. Kossowsky, R., Miller, D. G. and Diaz, E. S., Tensile and creep strengths of hot-pressed Si_3N_4. *J. Mater. Sci.,* 1975, **10**, 983–997.
32. Din, S. U. and Nicholson, P. S., Creep of hot-pressed silicon nitride. *J. Mater. Sci.,* 1975, **10**, 1375–1380.
33. Seltzer, M. S., High temperature creep of silicon-base compounds. *Am. Ceram. Soc. Bull.,* 1977, **56**, 418–423.
34. Arons, R. M. and Tien, J. K., Creep and strain recovery in hot-pressed silicon nitride. *J. Mater. Sci.,* 1980, **15**, 2046–2058.
35. Lange, F. F., Davis, B. I. and Clarke, D. R., Compressive creep of Si_3N_4/MgO alloys, part 1: effect of composition. *J. Mater. Sci.,* 1980, **15**, 601–610.
36. Lange, F. F. and Davis, B. I., Compressive creep of Si_3N_4/MgO alloys. *J. Mater. Sci.,* 1982, **17**, 3637–3640.
37. Crampon, J., Duclos, R. and Rakotoharisoa, N., Compression creep of $Si_3N_4/MgAl_2O_4$ alloys. *J. Mater. Sci.,* 1990, **25**, 1203–1208.
38. Todd, J. A. and Xu, Z. Y., The high temperature creep deformation of Si_3N_4–$6Y_2O_3$–$2Al_2O_3$. *J. Mater. Sci.,* 1989, **24**, 4443–4452.
39. Bodur, C. T., Effects of heat treatments on the creep properties of a hot pressed silicon nitride. *J. Mater. Sci.,* 1995, **30**, 1511–1515.
40. Ferber, M. K. and Jenkins, M. J., Evaluation of the strength and creep-fatigue behavior of hot isostatically pressed silicon nitride. *J. Am. Ceram. Soc.,* 1992, **75**, 2453–2462.
41. Ding, J.-L., Liu, K. C., More, K. L. and Brinkman, C. R., Creep and creep rupture of an advanced silicon nitride ceramic. *J. Am. Ceram. Soc.,* 1994, **77**, 867–874.
42. Ferber, M. K., Jenkins, M. J., Nolan, T. A. and Yeckley, R. L., Comparison of creep and creep rupture performance of two HIPed silicon nitride ceramics. *J. Am. Ceram. Soc.,* 1994, **77**, 657–665.